Entanglement scaling at first order quantum phase transitions

Published in:
New Journal of Physics

Document Version:
Publisher's PDF, also known as Version of record

Queen's University Belfast - Research Portal:
Link to publication record in Queen's University Belfast Research Portal

PAPER • OPEN ACCESS

Entanglement scaling at first order quantum phase transitions

To cite this article: A Yuste *et al* 2018 *New J. Phys.* **20** 043006

View the article online for updates and enhancements.

New Journal of Physics
The open access journal at the forefront of physics

CrossMark

PAPER

Entanglement scaling at first order quantum phase transitions

A Yuste[1], C Cartwright[2], G De Chiara[2] and A Sanpera[1,3]

[1] Física Teòrica: Informació i Fenòmens Quàntics, Departament de Física, Universitat Autònoma de Barcelona, 08193 Bellaterra, Barcelona, Spain
[2] Centre for Theoretical Atomic, Molecular, and Optical Physics, School of Mathematics and Physics, Queen's University Belfast, Belfast BT7 1NN, United Kingdom
[3] ICREA, Pg. Lluís Companys 23, E-08010, Barcelona, Spain

E-mail: abel.yuste@uab.cat

Keywords: entanglement, quantum phase transitions, spin chains, finite size scaling

Abstract

First order quantum phase transitions (1QPTs) are signalled, in the thermodynamic limit, by discontinuous changes in the ground state properties. These discontinuities affect expectation values of observables, including spatial correlations. When a 1QPT is crossed in the vicinity of a second order one, due to the correlation length divergence of the latter, the corresponding ground state is modified and it becomes increasingly difficult to determine the order of the transition when the size of the system is finite. Here we show that, in such situations, it is possible to apply finite size scaling (FSS) to entanglement measures, as it has recently been done for the order parameters and the energy gap, in order to recover the correct thermodynamic limit (Campostrini *et al* 2014 *Phys. Rev. Lett.* **113** 070402). Such a FSS can unambiguously discriminate between first and second order phase transitions in the vicinity of multicritical points even when the singularities displayed by entanglement measures lead to controversial results.

1. Introduction

Understanding how many-body interacting systems order into different quantum phases as well as the transitions between them remains one of the most challenging open problems in modern physics. Quantum phase transitions (QPTs) are associated with the non-analytical behavior of some observable and/or correlator which can be either local or non local. With the discovery of topological and new exotic phases [1], which fall outside Landau's symmetry breaking paradigm, the use of entanglement to describe quantum matter seems to be, by all means, necessary [2].

Here, we restrict ourselves to study entanglement behavior for a large class of QPTs which, in analogy to their classical counterparts, are signaled by singularities in the derivatives of the (free) energy [3]. In such cases, phase transitions are classified by the minimum order of the derivative of the ground state energy which is not continuous. Accordingly, first (1QPTs) and second (2QPTs) order QPTs show singular behavior on the first and second derivative of the ground state energy respectively. For 1QPTs, the singular behavior translates into abrupt discontinuities of some local observables while for 2QPTs the order parameters change continuously with a power law. In this last case, the thermodynamic limit can be recovered using finite size scaling (FSS) [4]. The scaling is characterized by the critical exponents allowing the classification of apparently different 2QPTs into the same universality class. With such definitions at hand it looks straightforward to distinguish if a given QPT is of first or second order. But this is not always the case when finite size effects are present. This question becomes especially relevant in the vicinity of multicritical points where several QPTs of different order coexist in a narrow range of Hamiltonian parameters.

First studies of the entanglement behavior close to a QPT were performed by analyzing bipartite entanglement in simple spin models like the quantum Ising spin-1/2 chain which exhibits a 2QPT. In [5, 6], the authors showed that, similarly to the ground state energy behavior, the bipartite entanglement between two adjacent spins, as measured by the concurrence, $\mathcal{C}$, has a derivative which diverges at the critical point in the thermodynamical limit.

Moreover, they showed that, for finite size systems, a FSS can be performed allowing the correct extraction of the critical exponents corresponding to the Ising transition. Since then, a large amount of work has been devoted to deepen the connections between quantum information and QPTs, see for instance [7–17].

In [18], the above results were generalized by using Kohn–Sham theorem which links ground state properties with reduced density matrices. For N-partite local Hamiltonians that contain at most k-body interactions, $\hat{H}(\lambda) = \sum_k \hat{H}_k(\lambda)$, where λ is a parameter in the Hamiltonian phase-space, such as the magnetization or an interaction strength. The energy of the ground state $|\Psi_0\rangle$ can be written as

$$E_0(\lambda) = \langle\Psi_0|\hat{H}|\Psi_0\rangle = \sum_k \mathrm{Tr}\ (\hat{H}_k\ \rho^k), \tag{1}$$

where ρ^k is the reduced density matrix acting on the local support of the corresponding local Hamiltonian $\hat{H}_k$. For the usual case of local Hamiltonians with just two-body interactions, $\hat{H}_k(\lambda) = \hat{H}_{ij}(\lambda)$, where the indexes i and j refer to two spins, it can be shown that $\partial_\lambda E_0 \sim (\partial_\lambda \hat{H}_{ij})\rho^{ij}$. If the local Hamiltonians are smooth functions of λ, then a one-to-one correspondence can be made between the singularities of $\partial_\lambda E_0(\lambda)$ arising in a 1QPT and the singularities of (the matrix elements of) ρ^{ij}. The above translates into discontinuous pairwise entanglement measures, which depend exclusively on ρ^{ij}. By the same reasoning, a singularity in $\partial_\lambda^2 E_0$, typical of a 2QPT, is associated to a singularity in the first derivative of the corresponding pairwise entanglement measure.

A theorem casting all the above results is stated in [18] claiming that, unless there exist accidental divergences, the order and properties of QPTs of local Hamiltonians are signalled by the entanglement measures associated to the corresponding reduced density matrix of the ground state. The theorem works in both directions, i.e. a discontinuity in a pairwise measure of entanglement in a 2-local Hamiltonian indicates a 1QPT while a discontinuity/divergence in its derivative signals a 2QPT. The above theorem has some known caveats. For instance, in the spin-1/2 XXZ chain, at the 1QPT between the ferromagnetic and critical phase, the concurrence is a function of the energy at the critical point and it remains continuous in the thermodynamic limit while its first derivative is discontinuous [19, 20]. For the same transition, it has been shown that a symmetry breaking in the ferromagnetic phase also modifies the origin of the non-analytic behavior of the concurrence [21]. In [22], a three-body local Hamiltonian model was presented in which the pairwise concurrence is non analytical in the absence of any QPT [22]. For 2D models even less is known.

Motivated by the above results, we analyze here scaling properties of pairwise entanglement measures for 2-local Hamiltonians near multicritical points. Although FSS is a tool to obtain the thermodynamical properties of the system for continuous (2QPT) phase transitions, here we show that such a tool can be employed also for entanglement measures for 1QPTs. Further, we demonstrate that when finite size effects are important, it is precisely the scaling of the entanglement measure and not the measure itself which determines the correct order of the transition. This fact is especially relevant for a 1QPT crossed in the vicinity of a 2QPT and it is in accordance with the recent results reported by Campostrini and coauthors [23] showing that the order parameter of a 1QPT can be continuous for finite systems and admits an appropriate FSS.

The paper is organized as follows. In section 2, we focus on the spin-1/2 Ising chain with longitudinal field and report how bipartite entanglement, as measured by e.g. the concurrence, scales in the 1QPT when is crossed near the multicritical point. This choice is motivated by the fact that this is an integrable model when the longitudinal field vanishes and serves as a playtool to analyze numerical results. In section 3, we move to a much more complex model, the spin-1 XXZ chain with uniaxial single-ion anisotropy. The phase diagram of the model is rich and has several QPTs whose boundaries are only known approximately. We focus on the 1QPT of the model and analyze by means of numerical techniques the behavior of bipartite entanglement in the vicinity of multicritical points. In section 4, we discuss the results and, finally, in section 5 we conclude.

2. Spin-1/2 Ising chain with longitudinal field

The first spin model we explore is the spin-1/2 Ising chain with a longitudinal field,

$$\hat{H} = -J\sum_{i=1}^{L-1} \hat{\sigma}_i^x \hat{\sigma}_{i+1}^x - B_z\sum_{i=1}^{L} \hat{\sigma}_i^z - B_x\sum_{i=1}^{L} \hat{\sigma}_i^x, \tag{2}$$

where L is the number of spins, $\hat{\sigma}_i^\alpha$ are the Pauli matrices for spin i and we set $J = 1$ and $B_z \geqslant 0$. In figure 1, we provide the phase diagram of the model. For $B_x = 0$, where the system reduces to the integrable Ising model, there is a 2QPT at $B_z = 1$ between the ferromagnetic ($B_z < 1$) and paramagnetic phases ($B_z > 1$). This 2QPT was the first one studied by means of bipartite entanglement [5]. When $B_x \neq 0$, the system is no longer integrable and we obtain the ground state of the system using both, the density matrix renormalization group (DMRG) with open boundary conditions (OBCs) [24–26] and exact diagonalization (ED) calculations. When the system is in the ferromagnetic phase, a 1QPT takes place at $B_x = 0$ between the two ferromagnetic ground states, ferromagnetic ↑ and ferromagnetic ↓. This transition can be detected by a discontinuity in the magnetization,

Figure 1. Phase diagram for the spin-1/2 Ising chain with a longitudinal field. The dashed line (- - -) depicts the 1QPT while the dotted line (...) the 2QPT.
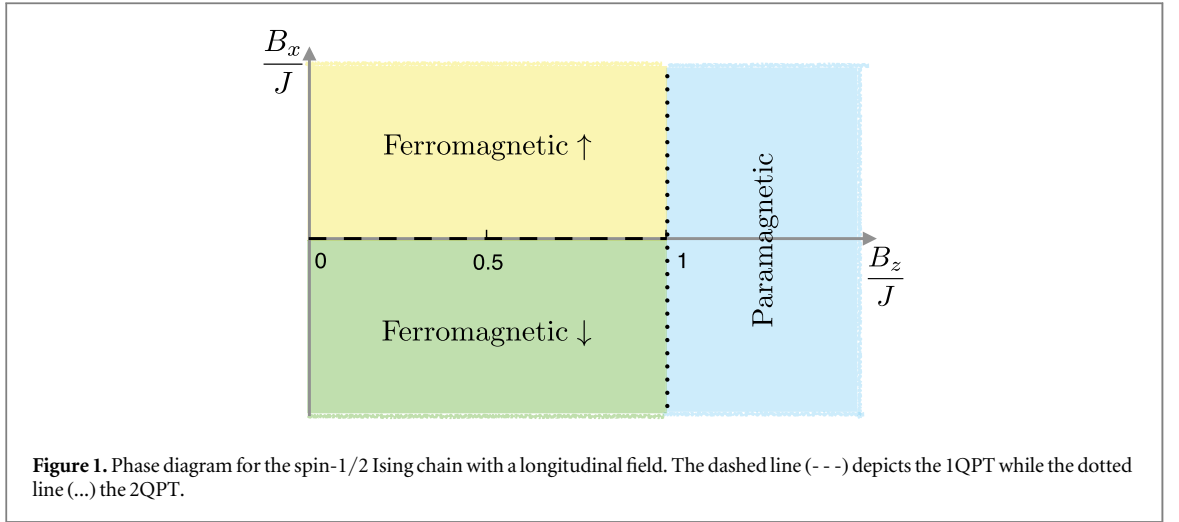
$M_x = \sum_i \langle \hat{\sigma}_i^x \rangle$, which passes from positive to negative values. However, for finite systems, numerical calculations in a region sufficiently close to $B_x = 0$ show a smooth slope in M_x instead of a discontinuity. To deal with this effect, in [23] a FSS is proposed for first order quantum transitions in a chain of size L driven by a magnetic field h. There, on dimensional grounds, it is argued that around the critical point ($h = 0$), if there is scaling behavior, the relevant scaling variable, κ, should correspond to the ratio between the energy contribution of h, and the gap at the critical point, $\Delta_L = \Delta_L(L, h = 0)$,

$$\kappa \sim \frac{hL}{\Delta_L}. \tag{3}$$

As a result, heuristically when $hL \sim \Delta_L$, the ground state energy becomes effectively continuous along the transition and so does the order parameter. This feature becomes more relevant the closer the critical point is to a 2QPT, since the correlation length of the system (ξ) diverges, enhancing the nearby finite size effects. In [23], it is shown that across the 1QPT of the longitudinal Ising chain (equation (2)) occurring at $B_x = 0$, the first energy gap and the magnetization obey the following scaling ansatz:

$$\Delta(L, B_x) \approx \Delta_L f_\Delta(\kappa), \tag{4}$$

$$M_x(L, B_x) \approx m_0 f_M(\kappa), \tag{5}$$

where $f_\Delta(\kappa)$ and $f_M(\kappa)$ are continuous universal functions for all L and B_z. Since the model is integrable for $B_x = 0$, the scaling variable can be defined as [23]

$$\kappa_1 = \frac{2m_0 B_x L}{\Delta_L}, \tag{6}$$

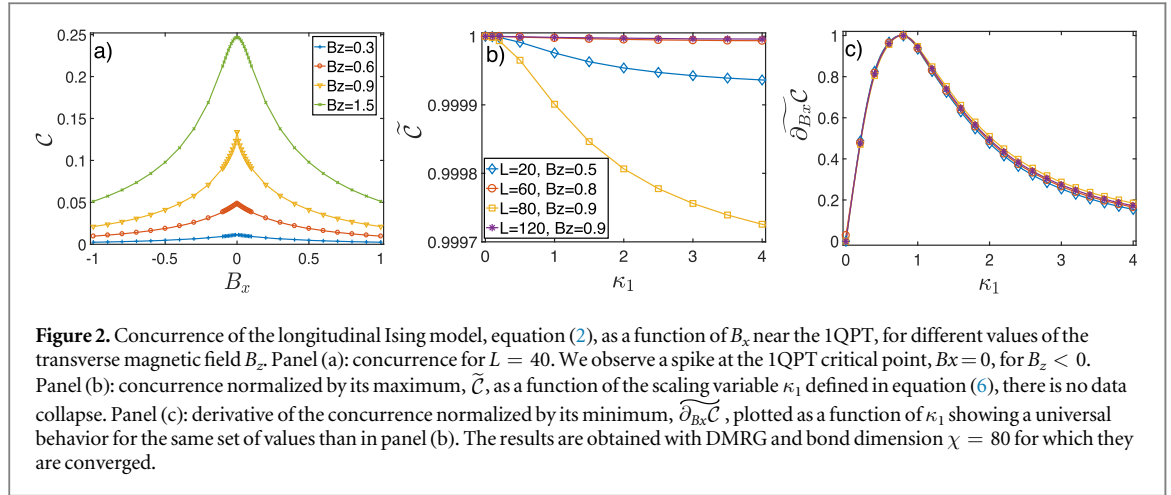where $\Delta_L = \Delta_{L, B_x=0} \approx 2(1 - B_z^2)B_z^L$, is the first gap at the critical point, $B_x = 0$ for OBC and

$$m_0 = \lim_{B_x \to 0^+} \lim_{L \to \infty} \langle \hat{\sigma}_x \rangle = (1 - B_z^2)^{1/8}. \tag{7}$$

Clearly, as one approaches the critical point, $B_x = 0$, in the nearby region of the 2QPT ($B_z = 1$), the gap closes and even at very small values of the driving parameter B_x around the critical point, the 1QPT transition looks continuous. Here, we apply the above scaling concepts to the entanglement across the 1QPT transition. Since the Hamiltonian is 2-local, discontinuities in entanglement measures have to be related to two-body (pairwise) entanglement of two nearest-neighbor spins (i, j) described by the reduced density matrix, ρ^{ij}. For pure states, all measures of bipartite entanglement are in one-to-one correspondence and are all a function of the eigenvalues of the reduced density matrix arising from the chosen partition. For mixed states, this is not the case anymore and the entanglement measure has to be calculated as the convex roof of the corresponding pure state measure. An exception for mixed states ρ of two spin-1/2 particles or qubits, is the concurrence [27] which is equivalent to the entanglement cost and has a closed analytical expression:

$$\mathcal{C}(\rho) = \max(0, \lambda_1 - \lambda_2 - \lambda_3 - \lambda_4), \tag{8}$$

where λ_i are the eigenvalues, in decreasing order, of the matrix $R = \sqrt{\sqrt{\rho}\tilde{\rho}\sqrt{\rho}}$ with $\tilde{\rho} = (\hat{\sigma}_y \otimes \hat{\sigma}_y)\rho^*(\hat{\sigma}_y \otimes \hat{\sigma}_y)$, where the product $\hat{\sigma}_y \otimes \hat{\sigma}_y$ is defined in the Hilbert space of the two spins and ρ^* is the complex conjugate of ρ. Since $\mathcal{C}$ is supposed to be discontinuous at the critical point for 1QPTs, naively we might expect that it will follow a similar scaling behavior as M_x, equation (5). In figure 2, we show $\mathcal{C}$ for the two central spins which, if border effects are neglected, will also hold for the rest of neighboring spin pairs. In the left panel, we observe that $\mathcal{C}$ is a continuous function with a spike at the critical point which signals a singularity in the first derivative, $\partial_{B_x}\mathcal{C}$. The

Figure 2. Concurrence of the longitudinal Ising model, equation (2), as a function of B_x near the 1QPT, for different values of the transverse magnetic field B_z. Panel (a): concurrence for $L = 40$. We observe a spike at the 1QPT critical point, $Bx = 0$, for $B_z < 0$. Panel (b): concurrence normalized by its maximum, $\widetilde{\mathcal{C}}$, as a function of the scaling variable κ_1 defined in equation (6), there is no data collapse. Panel (c): derivative of the concurrence normalized by its minimum, $\widetilde{\partial_{Bx}\mathcal{C}}$, plotted as a function of κ_1 showing a universal behavior for the same set of values than in panel (b). The results are obtained with DMRG and bond dimension $\chi = 80$ for which they are converged.

spike becomes more pronounced as the transition gets closer to the 2QPT at $B_z = 1$. It is worth pointing out that such a behavior bears strong similarities with the geometric entanglement, a collective measure of entanglement indicating how much the ground state differs from a separable state [14]. Notice that for $B_z > 1$, when the system is in the paramagnetic phase independently of the sign of the longitudinal field B_x, (as indicated in figure 2 for $B_z = 1.5$), the concurrence becomes a smooth function of B_x. In the central panel of figure 2, we plot the scaling of the concurrence normalized by its maximum value, $\widetilde{\mathcal{C}} = \mathcal{C}/\mathcal{C}_{\max}$, as a function of the scaling variable κ_1 to determine whether $\mathcal{C}$ fulfills a similar scaling relation as in equation (5). It is enough to investigate what happens for $\kappa_1 > 0$ because $\mathcal{C}(\kappa_1)$ has even parity, i.e. $\mathcal{C}(\kappa_1) = \mathcal{C}(-\kappa_1)$. This is a consequence of the Hamiltonian, and, therefore, the ground state, being invariant under the change $B_x \to -B_x$ and a local π-rotation of the spins around the z-axis. Finally, in panel c) we display the scaling of the derivative of the concurrence normalized by its minimum value $\widetilde{\partial_{Bx}\mathcal{C}} = \partial_{Bx}\mathcal{C}/[\partial_{Bx}\mathcal{C}]_{\min}$. Interestingly enough, the concurrence does not scale with the fitting parameter κ_1, but its derivative does. In the central panel, we can see that the data for different B_z and L do not collapse in a universal function, while, in the right panel, there is a good data collapse for different values of B_z and L. Thus, $\partial_{Bx}\mathcal{C}$ fulfills the scaling ansatz,

$$\partial_{Bx}\mathcal{C}(L, B_z) = [\partial_{Bx}\mathcal{C}]_{\min} g(\kappa_1), \tag{9}$$

where $g(\kappa_1)$ is a universal function for any L and B_z. We further discuss all these results in section 4.

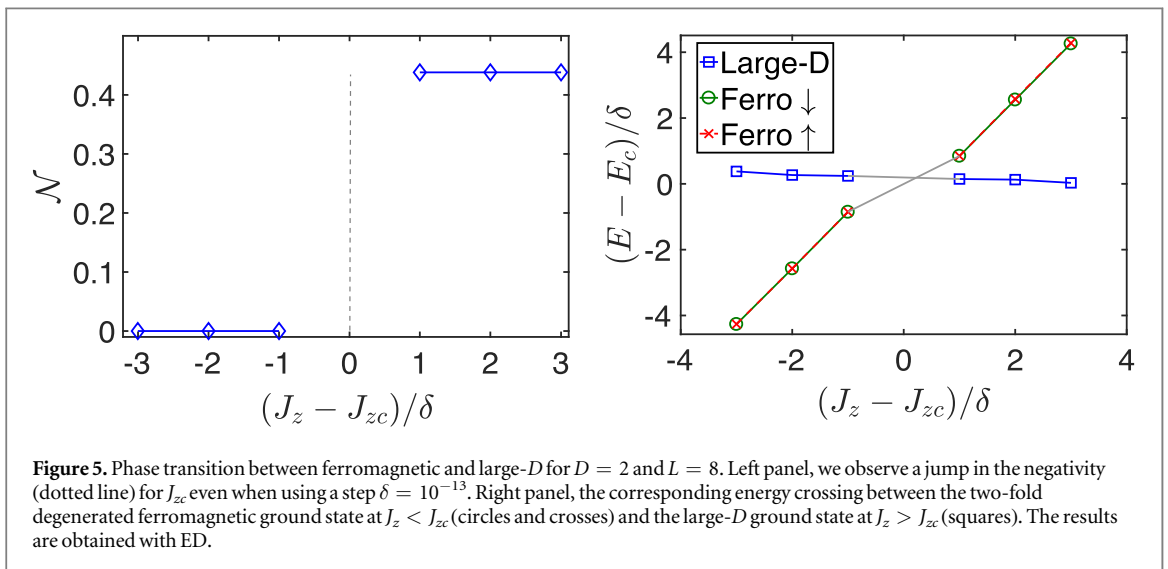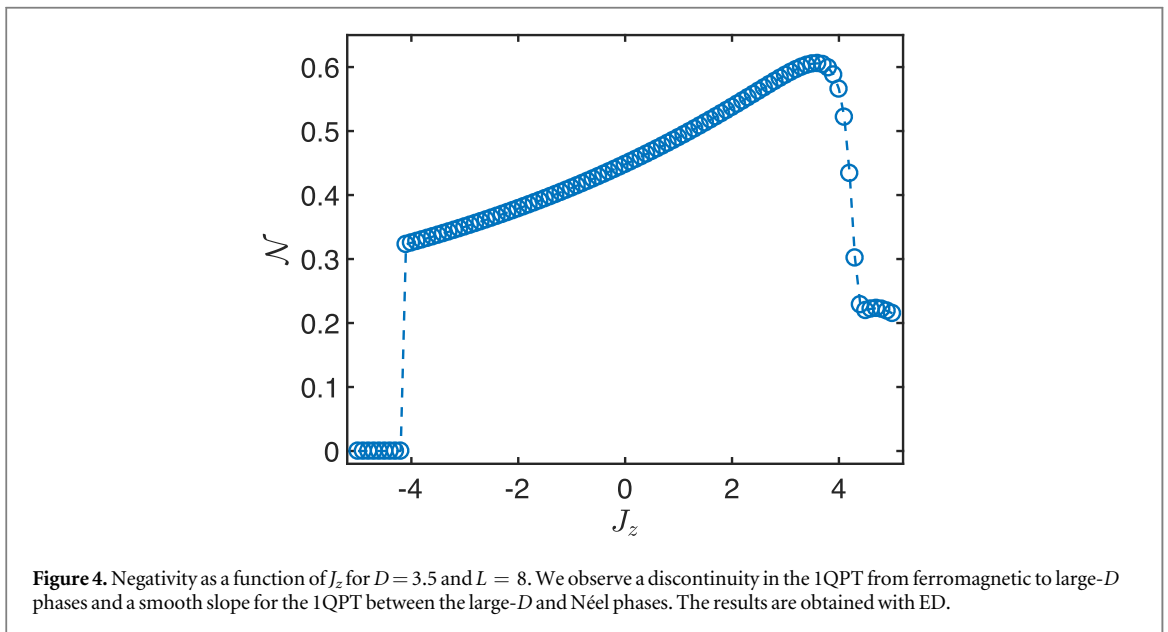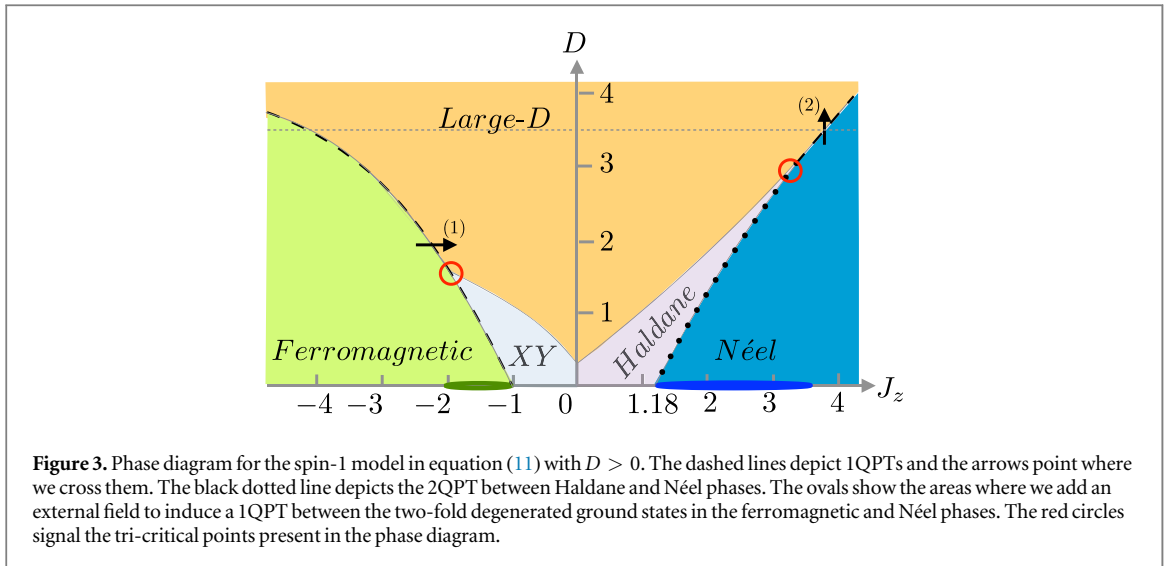## 3. Spin-1 XXZ chain with uniaxial single-ion anisotropy

In this section, we extend the study of entanglement along 1QPTs to a spin-1 system. Since the concurrence, $\mathcal{C}$, can only be easily computed for the mixed states of qubits, in order to compute the entanglement between two spin-1 particles we use the negativity [28, 29]

$$\mathcal{N}(\rho) = \frac{||\rho^{T_B}||_1 - 1}{2}, \tag{10}$$

where the operation T_B is the partial transpose defined now on the reduced density matrix of two nearest neighbors spins, ρ^{ij}, and $||...||_1$ is the sum of the absolute value of all singular values. Notice that negativity is a lower bound to entanglement. The model under scrutiny is the spin-1 XXZ chain with uniaxial single-ion anisotropy,

$$\hat{H} = \sum_{l=1}^{L-1} [J\hat{S}_l^x \hat{S}_{l+1}^x + J\hat{S}_l^y \hat{S}_{l+1}^y + J_z \hat{S}_l^z \hat{S}_{l+1}^z] + D\sum_{l=1}^{L} (\hat{S}_l^z)^2, \tag{11}$$

where $\hat{S}_l^\alpha$ are the spin-1 matrices for spin l and D is the uniaxial single-ion anisotropy which we take as positive. We set $J = 1$, and use it as the unit of energy. We choose this model because of the richness of its phase diagram [30], schematically shown in figure 3, with several 1QPTs which we depict with dashed lines. The behavior of $\mathcal{N}$ along the different 1QPTs present in the model is very different depending on their closeness to a multicritical point which also involves 2QPTs. We start by examining the negativity as a function of the J_z for a constant uniaxial field $D = 3.5$ and $L = 8$. Two 1QPTs are crossed at such value of D, as indicated in the phase diagram by a gray horizontal line (see figure 3). The first one corresponds to the transition from ferromagnetic order to the large-D phase, which is crossed approximately at $J_z = -4.2$. Another 1QPT appears between large-D/Néel at approximately $J_z = 3.8$. As clearly shown in figure 4, the former phase transition is clearly signalled by a discontinuity in $\mathcal{N}$, whereas the latter shows a smooth slope along the transition. In figure 5, we show in detail

Figure 3. Phase diagram for the spin-1 model in equation (11) with $D > 0$. The dashed lines depict 1QPTs and the arrows point where we cross them. The black dotted line depicts the 2QPT between Haldane and Néel phases. The ovals show the areas where we add an external field to induce a 1QPT between the two-fold degenerated ground states in the ferromagnetic and Néel phases. The red circles signal the tri-critical points present in the phase diagram.

Figure 4. Negativity as a function of J_z for $D = 3.5$ and $L = 8$. We observe a discontinuity in the 1QPT from ferromagnetic to large-D phases and a smooth slope for the 1QPT between the large-D and Néel phases. The results are obtained with ED.

Figure 5. Phase transition between ferromagnetic and large-D for $D = 2$ and $L = 8$. Left panel, we observe a jump in the negativity (dotted line) for J_{zc} even when using a step $\delta = 10^{-13}$. Right panel, the corresponding energy crossing between the two-fold degenerated ferromagnetic ground state at $J_z < J_{zc}$ (circles and crosses) and the large-D ground state at $J_z > J_{zc}$ (squares). The results are obtained with ED.

Figure 6. Left column: negativity. Right column: staggered magnetization. Results are for $J_z = 3.8$ and different L. In the first row, we plot the quantities as a function of D. We observe a smooth slope of both the negativity and the staggered magnetization where the 1QPT is expected. Bottom row, quantities plotted as a function of κ_2 showing the tendency to converge towards a universal function. The results are obtained with DMRG and bond dimension $\chi = 150$ for which they are converged.
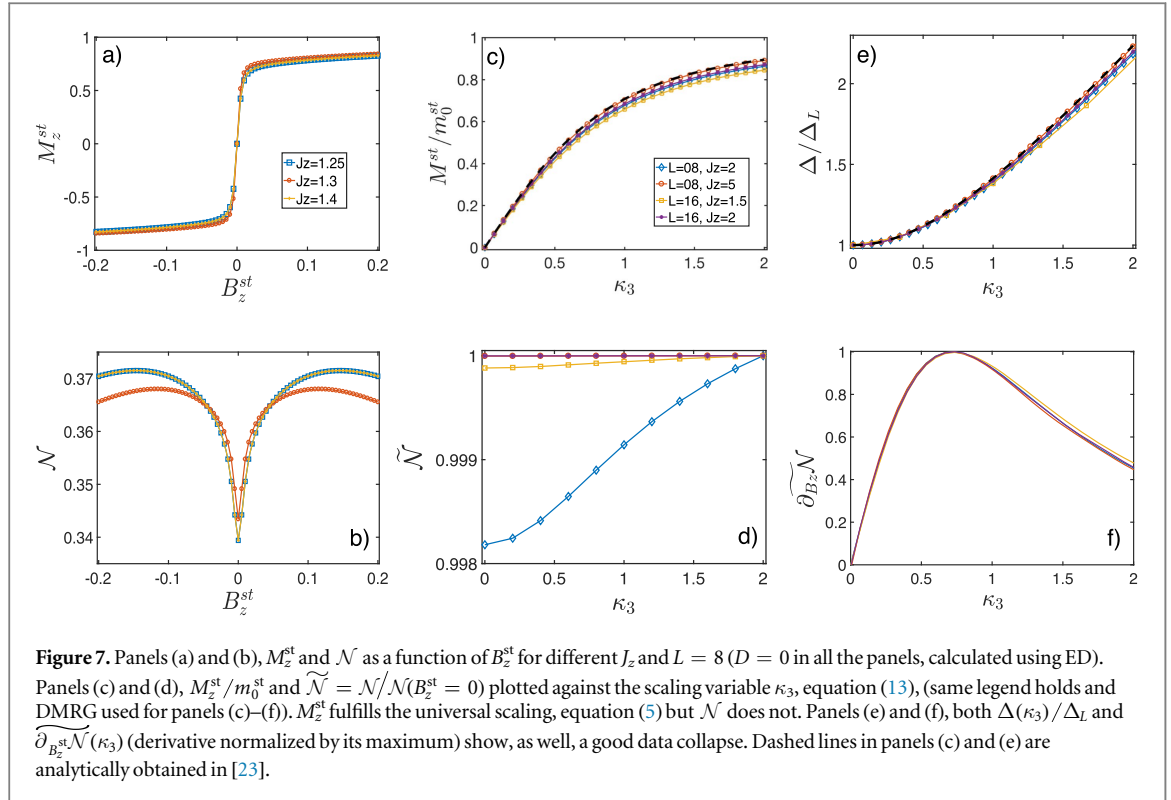
the generic behavior of $\mathcal{N}$ together with the corresponding level crossing along the ferromagnetic/large-D phase transition. We cross the transitions at a fixed value $D = 2$, as depicted by (1) in figure 3, in the nearby region of a critical point (depicted by a red circle). We observe that even for small steps of the parameter J_z driving the 1QPT, $\mathcal{N}$ is always discontinuous and a neat level crossing is shown between the two-fold degenerated ferromagnetic ground state, for $J_z < J_{zc}$, and the large-D ground state, for $J_z > J_{zc}$. This means that, at J_{zc}, there is a sudden change in the ground state which is detected by a discontinuity in $\mathcal{N}$. Therefore, in figure 5, we observe the expected discontinuous behavior for $\mathcal{N}$ along a 1QPT even for a system of just 8 spins without any finite size effects.

We focus now on to the large-D/Néel 1QPT. In figure 6 we display the negativity and the staggered magnetization for a fixed value $J_z = 3.8$ as a function of the anisotropy, D, around the critical point $D_{c,L}$ denoted by (2) in figure 3. We add the subindex L to indicate that this quantity now depends on the system size. In order to show the behavior for larger systems, we use DMRG calculations for $L = 32, 64, 128$ and 150. In the two top panels, we observe that both, $\mathcal{N}$ and the staggered magnetization, $M_z^{st} = \sum_{i=1}^{L}(-1)^i \langle \hat{S}_i^z \rangle$, change smoothly around the transition point. As L increases, the slope becomes more pronounced getting closer to a discontinuity and we need values of D closer to the critical point to observe the continuous slope. For instance, the necessary step in D to observe a continuous behavior is $\delta \sim 10^{-4}$ and $\delta \sim 10^{-6}$ for $L = 64$ and $L = 150$, respectively. Note that in this case, as in section 2, we are very close to a 2QPT. As we get further from the tricritical point, i.e. as we increase the value to $J_z \gg J_{crit} = 3.8$, this effect progressively becomes less important and both $\mathcal{N}$ and M_z^{st} are effectively discontinuous. Since the transition is known to be of first order, we propose a similar FSS as in the previous section, defining a relevant scaling variable, κ_2, as the ratio between the energy contribution of D along the transition and the gap at the critical point,

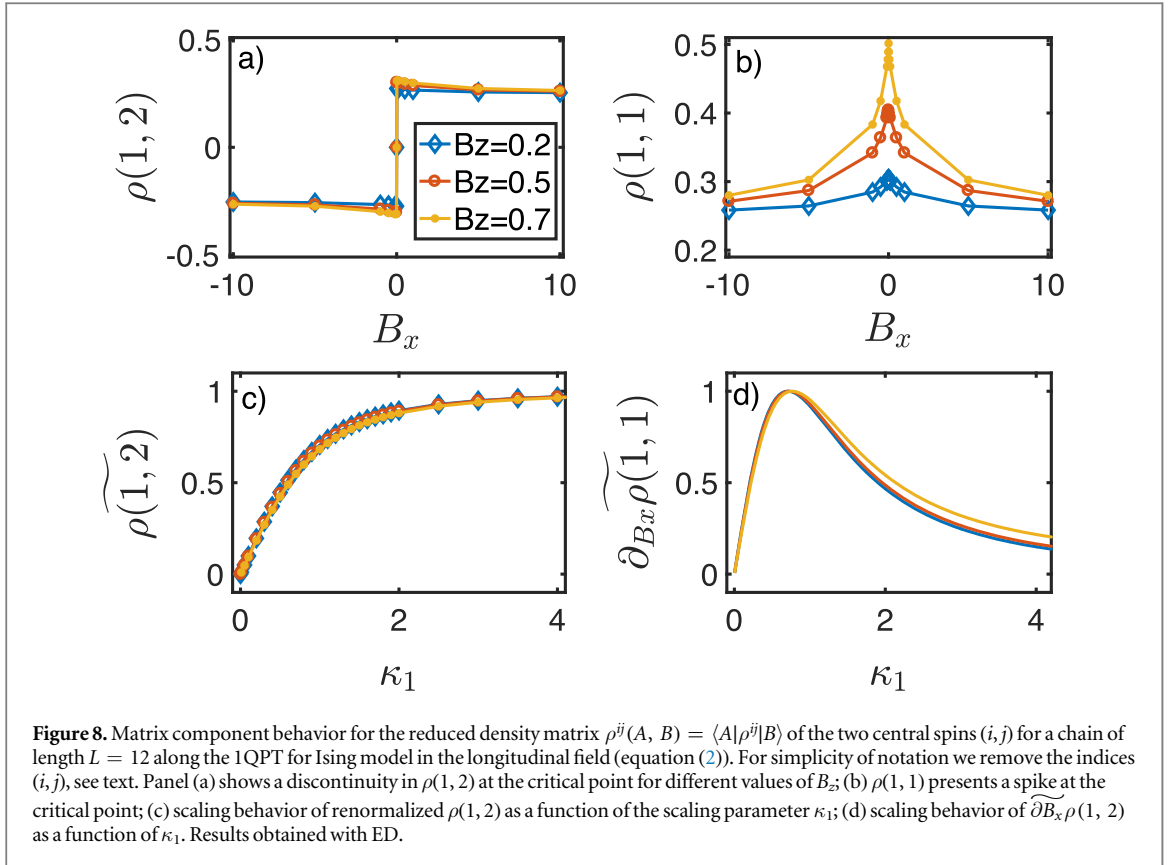$$\kappa_2 \sim \frac{(D - D_{c,L})L}{\Delta_L}. \tag{12}$$

Now, Δ_L is obtained numerically and $(D - D_{c,L})L$ is a bare estimation for the energy contribution of the parameter D. In the bottom panels, we plot $\mathcal{N}$ and M_z^{st} as a function of this scaling variable κ_2. As we can observe, both quantities seem to converge, though not perfectly, towards a universal scaling, as described by equation (5). It is worth mentioning that equation (12) is an approximation whereas, in the previous section we had analytic expressions for Δ_L and m_0 in equation (6). Actually, in [31], a similar FSS, with non-analytic expressions, is proposed for the Potts chain with a similar convergence. It seems reasonable, thus, to state that for this 1QPT, when we are close to the 2QPT, $\mathcal{N}$ is continuous due to finite size effects and that it obeys the scaling ansatz for 1QPT.

Figure 7. Panels (a) and (b), M_z^{st} and $\mathcal{N}$ as a function of B_z^{st} for different J_z and $L = 8$ ($D = 0$ in all the panels, calculated using ED). Panels (c) and (d), M_z^{st}/m_0^{st} and $\widetilde{\mathcal{N}} = \mathcal{N}/\mathcal{N}(B_z^{st} = 0)$ plotted against the scaling variable κ_3, equation (13), (same legend holds and DMRG used for panels (c)–(f)). M_z^{st} fulfills the universal scaling, equation (5) but $\mathcal{N}$ does not. Panels (e) and (f), both $\Delta(\kappa_3)/\Delta_L$ and $\widetilde{\partial_{B_z^{st}}\mathcal{N}}(\kappa_3)$ (derivative normalized by its maximum) show, as well, a good data collapse. Dashed lines in panels (c) and (e) are analytically obtained in [23].

Finally, we analyze the behavior of $\mathcal{N}$ when the 1QPT is due to a $\mathbb{Z}_2$ symmetry breaking of a two fold-degenerated ground state. To this aim we add an extra magnetic field, $B_z \sum_{i=1}^{L} \hat{S}_i^z$ (extra magnetic staggered field $B_z^{st} \sum_{i=1}^{L} (-1)^i \hat{S}_i^z$) in the ferromagnetic (Néel) phase of the XXZ spin-1 model in equation (11). These new terms lead to two new 1QPT between ferromagnetic ↑ / ferromagnetic ↓ (Néel/Anti Néel) phases, depicted graphically by ovals along $D = 0$ line in the phase diagram of the model (see figure 3). The corresponding order parameter for both transitions, the magnetization (M_z), and the staggered magnetization (M_z^{st}) respectively, are discontinuous in the thermodynamic limit. For the first induced QPT between the ferromagnetic phases, the entanglement remains always constant and zero. More interesting features appear in the Néel/Anti-Néel transition whose results are summarized in figure 7. These results are obtained using a mixture of ED (panels (a) and (b)) and DMRG (in the remaining panels). The bond dimension in DMRG was chosen in such a way that the results converged, which meant using a bond dimension of 100 or 150. In panels (a) and (b) we show, respectively, M_z^{st} and $\mathcal{N}$ as a function of the added staggered magnetic field B_z^{st}. While the order parameter, M_z^{st}, has the expected discontinuous behavior, the pairwise entanglement, $\mathcal{N}$, has a dip at the critical point, displaying a continuous $\mathcal{N}$ but a discontinuous derivative. In order to apply the proper FSS ansatz for the negativity, we start by defining first the relevant scaling variable (as we did in section 2):

$$\kappa_3 = \frac{2m_0^{st} B_z^{st} L}{\Delta_L}. \tag{13}$$

In full analogy with the results presented in section 2, and due to the fact that the 2QPT between Haldane/Néel phases belongs to the same universality class as the spin-1/2 Ising, we use the expression of m_0^{st} from equation (7) by substituting $B_z \rightarrow J_{zc}/J_z$, where $J_{zc} \approx 1.186$ corresponds the 2QPT critical point for $D = 0$ [32]. Our scaling results are summarized in panels (c) and (d) of figure 7, where we show, respectively, M_z^{st} and $\mathcal{N}$ as a function of κ_3. The scaling ansatz, equation (5), works properly for M_z^{st}, but, as it happens for the concurrence, $\mathcal{C}$, in the spin-1/2 Ising chain, the scaling also fails for the negativity $\mathcal{N}$ in this phase transition. Finally, in panels (e) and (f) we show how the gap, Δ_L, fulfills the scaling ansatz, equation (4), and how the derivative of the negativity, $\partial_{B_z^{st}} N$, also verifies the scaling ansatz, equation (9). This last behavior strongly resembles the behavior of the derivative on the concurrence for the spin longitudinal Ising spin 1/2 chain. To further ensure the correctness of our results, in figure 7 we also display the comparison between our numerical data, $M^{st}(\kappa_3)$ and $\Delta_L(\kappa_3)$, with the analytic expressions using an effective two level theory as derived in [23].

Figure 8. Matrix component behavior for the reduced density matrix $\rho^{ij}(A, B) = \langle A|\rho^{ij}|B\rangle$ of the two central spins (i, j) for a chain of length $L = 12$ along the 1QPT for Ising model in the longitudinal field (equation (2)). For simplicity of notation we remove the indices (i, j), see text. Panel (a) shows a discontinuity in $\rho(1, 2)$ at the critical point for different values of B_z; (b) $\rho(1, 1)$ presents a spike at the critical point; (c) scaling behavior of renormalized $\rho(1, 2)$ as a function of the scaling parameter κ_1; (d) scaling behavior of $\widetilde{\partial_{B_x}}\rho(1, 2)$ as a function of κ_1. Results obtained with ED.

4. Results discussion

Let us discuss here the origin of the concurrence's continuity together with its discontinuous first derivative across the the 1QPT in the spin-1/2 Ising model described in equation (2). A similar response is shown by the negativity in the spin-1 XXZ chain across the 1QPT between the Nèel/Anti-Néel phases. These transitions apparently contradict the expected behavior stated in [18] that links a singularity in the first derivative of the pairwise entanglement to a 2QPT, given that this singularity originates exclusively from the elements of ρ^{ij}, in equation (1). To determine the origin of this unusual behavior, we focus on the Ising longitudinal model and analyze the elements of the reduced density matrix of the two central spins (ij) that we denote by $\rho(A, B) \equiv \langle A|\rho^{ij}|B\rangle$ as a function of longitudinal field, B_x, for different values of the transverse magnetic field B_z. For simplicity of notation we remove from now on the super indices i, j. Given the symmetries of the Hamiltonian, it suffices to consider just two different matrix elements, $\rho(1, 1) = \langle \uparrow \uparrow |\rho^{ij}| \uparrow \uparrow\rangle$ and $\rho(1, 2) = \langle \uparrow \uparrow |\rho^{ij}| \downarrow \uparrow\rangle$, for analyzing the behavior of the concurrence. As plotted in the top panels of figure 8, $\rho(1, 2)$ is discontinuous along the 1QPT transition, while $\rho(1, 1)$ presents a spike signalling a singularity in its first derivative. In the bottom panels, we display our results regarding their scaling behavior as a function of the relevant scaling parameter κ_1 (see equation (6)). Interestingly enough, as shown in panel (c), the matrix element $\rho(1, 2)$ follows exactly the same scaling proposed for 1QPT [23], while it is derivative of the matrix element $\rho(1, 1)$ ($\partial_{B_x}\rho(1, 1)$) and not the matrix element itself which scales properly for different values of L and B_z. Furthermore, it can be shown that all the discontinuities present in elements such as $\rho(1, 2)$ cancel out when computing the concurrence. As a result, the concurrence $\mathcal{C}$ shows a singularity in the first derivative as it would happen in a 2QPT and it is precisely $\partial_{B_x}\mathcal{C}$ the quantity which fulfills the FSS and not $\mathcal{C}$ itself. The same analysis applies to the spin-1 XXZ chain with on-site anisotropy, where a dip in the negativity, $\mathcal{N}$, at the critical point appears. This behavior has the same origin as the previously reported spin-1/2 case and, therefore, it is the derivative of $\mathcal{N}$ and not the negativity itself which fulfills the FSS for 1QPTs. Hence, in these cases, a singularity in the first derivative of the concurrence/negativity (given and the concurrence/negativity are continuous functions), does not signal a 2QPT as it was conjectured in [18].

5. Conclusions

In conclusion, in this work we have analyzed pairwise entanglement behavior in diverse 1QPT transitions driven by 2-local Hamiltonians. We have shown the dramatic importance of finite size effects when 1QPT occur in the

nearby region of multicritical point containing also 2QPT. To illustrate this fact, we have shown examples of 1QPT in 2-body-Hamiltonians in which pairwise entanglement measures are continuous across the phase transition while their first derivatives are not. We have extended our results by using non integrable models in which the same behavior can be observed. A deeper analysis shows that the behavior is inherited from the two body reduced density matrix elements, which for 2-local Hamiltonians, are linked to the non-analyticities of the ground state energy. Our main result has been to demonstrate that for finite systems, the order of the QPT in symmetry broken phases is given by the scaling behavior of their bipartite entanglement and not by its non-analytical character. Our results should allow to better determine the order and boundaries of QPTs near multicritical points.

Acknowledgments

ORCID iDs

G De Chiara ● https://orcid.org/0000-0003-3265-9021

References

[1] Kosterlitz J M and Thouless D J 1973 *J. Phys. C: Solid State Phys.* **6** 1181
[2] Amico L, Fazio R, Osterloh A and Vedral V 2008 *Rev. Mod. Phys.* **80** 517–76
[3] Sachdev S 2001 *Quantum Phase Transitions* (Cambridge: Cambridge University Press)
[4] Fisher M E and Barber M N 1972 *Phys. Rev. Lett.* **28** 1516–9
[5] Osterloh A, Amico L, Falci G and Fazio R 2002 *Nature* **416** 608–10
[6] Osborne T J and Nielsen M A 2002 *Phys. Rev.* A **66** 032110
[7] Bose I and Chattopadhyay E 2002 *Phys. Rev.* A **66** 062320
[8] Vidal G, Latorre J I, Rico E and Kitaev A 2003 *Phys. Rev. Lett.* **90** 227902
[9] Latorre J I, Rico E and Vidal G 2004 *Quantum Inf. Comput.* **4** 48–92 (arXiv: quant-ph/0304098)
[10] Vidal J, Palacios G and Mosseri R 2004 *Phys. Rev.* A **69** 022107
[11] Alcaraz F C, Saguia A and Sarandy M S 2004 *Phys. Rev.* A **70** 032333
[12] Vidal J, Mosseri R and Dukelsky J 2004 *Phys. Rev.* A **69** 054101
[13] Barnum H, Knill E, Ortiz G, Somma R and Viola L 2004 *Phys. Rev. Lett.* **92** 107902
[14] Orús R and Wei T C 2010 *Phys. Rev.* B **82** 155120
[15] Gu S J, Lin H Q and Li Y Q 2003 *Phys. Rev.* A **68** 042330
[16] Stasińska J, Rogers B, Paternostro M, De Chiara G and Sanpera A 2014 *Phys. Rev.* A **89** 032330
[17] Hofmann M, Osterloh A and Gühne O 2014 *Phys. Rev.* B **89** 134101
[18] Wu L A, Sarandy M S and Lidar D A 2004 *Phys. Rev. Lett.* **93** 250404
[19] Gu S J, Lin H Q and Li Y Q 2003 *Phys. Rev.* A **68** 042330
[20] Syljuåsen O F 2003 *Phys. Rev.* A **68** 060301
[21] Pereira L J and de Oliveira T R 2016 *Front. Phys.* **4** 51
[22] Yang M F 2005 *Phys. Rev.* A **71** 030302
[23] Campostrini M, Nespolo J, Pelissetto A and Vicari E 2014 *Phys. Rev. Lett.* **113** 070402
[24] White S R 1992 *Phys. Rev. Lett.* **69** 2863–6
[25] White S R 1993 *Phys. Rev.* B **48** 10345–56
[26] De Chiara G, Rizzi M, Rossini D and Montangero S 2008 *J. Comput. Theor. Nanosci.* **5** 1277–88
[27] Hill S and Wootters W K 1997 *Phys. Rev. Lett.* **78** 5022–5
[28] Życzkowski K, Horodecki P, Sanpera A and Lewenstein M 1998 *Phys. Rev.* A **58** 883–92
[29] Vidal G and Werner R F 2002 *Phys. Rev.* A **65** 032314
[30] Chen W, Hida K and Sanctuary B C 2003 *Phys. Rev.* B **67** 104401
[31] Campostrini M, Nespolo J, Pelissetto A and Vicari E 2015 *Phys. Rev.* E **91** 052103
[32] Ejima S and Fehske H 2015 *Phys. Rev.* B **91** 045121